wafers using a hydrothermal method. Electron microscopy shows the tubes to have outer diameters of 20–40 nm and wall thicknesses in the range 5–15 nm. HRTEM images and SAED analysis shows the tubes to be single-crystalline. Annealing the nanotube arrays in vacuum, at low (300 °C) temperature, causes substantial enhancement of the UV PL following 325 nm excitation, and much reduced green–yellow emission.

Experimental

Thin-ZnO-film-coated Si wafers were used as substrates for subsequent growth of nanorod and nanotube arrays. The ZnO thin films were formed via PLD (with the T_{sub} in the range 25–450 °C, and deposition times of 1–45 min). The PLD system has been described elsewhere [22]. 50 mL of 0.1 M aqueous solutions of zinc nitrate (Alfa Aesar, 99 %) and methenamine (Alfa Aesar, 99+ %) were each maintained at constant temperature (90 °C) using a thermostatically controlled oil bath, and then mixed in a sealed glass bottle. For nanorod growth, and the growth of nanotubes on nanorods, the substrates were immersed in the reactive solution immediately after mixing. Typical growth times were $t < 3$ h for nanorod arrays, and $t > 6$ h for the growth of nanotubes on nanorods. The highest-density nanorod/nanotube arrays were grown on very thin ZnO template layers (1–5 min deposition time) on Si. These substrates were pre-heated (to ~ 90 °C) and immersed in the reactive solution that had been previously maintained at 90 °C for a user-selected time $\tau = 10$–60 h after mixing. The as-grown samples were rinsed in deionized water, and then dried in air at room temperature. Deposited products were characterized and analyzed using SEM (JEOL 6300 LV), TEM (JEOL 1200EX), and HRTEM (JEOL 2010). PL spectra were measured at room temperature following excitation with a continuous-wave He–Cd laser ($\lambda = 325$ nm, power ~ 3 mW).

Received: April 9, 2005
Final version: May 25, 2005
Published online: August 22, 2005

[1] S. Iijima, *Nature* **1991**, *354*, 56.
[2] J. Li, Y. J. Lu, Q. Ye, M. Cinke, J. Han, M. Meyyappan, *Nano Lett.* **2003**, *3*, 929.
[3] D. T. Mitchell, S. B. Lee, L. T. Trofin, N. Li, T. K. Nevanen, H. Soderlund, C. R. Martin, *J. Am. Chem. Soc.* **2002**, *124*, 11 864.
[4] J. Lawrence, G. Xu, *Appl. Phys. Lett.* **2004**, *84*, 918.
[5] N. W. S. Kam, T. C. Jessop, P. A. Wender, H. J. Dai, *J. Am. Chem. Soc.* **2004**, *126*, 6850.
[6] M. Zamfirescu, A. Kavokin, B. Gil, G. Malpuech, M. Kaliteevski, *Phys. Rev. B* **2002**, *65*, 161 205.
[7] C. J. Lee, T. J. Lee, S. C. Lyu, Y. Zhang, H. Ruh, H. J. Lee, *Appl. Phys. Lett.* **2002**, *81*, 3648.
[8] H. Yumoto, T. Inoue, S. J. Li, T. Sako, K. Nishiyama, *Thin Solid Films* **1999**, *345*, 38.
[9] E. Comini, G. Faglia, G. Sberveglieri, Z. W. Pan, Z. L. Wang, *Appl. Phys. Lett.* **2002**, *81*, 1869.
[10] B. P. Zhang, N. T. Binh, K. Wakatsuki, Y. Segawa, Y. Yamada, N. Usami, M. Kawasaki, H. Koinuma, *Appl. Phys. Lett.* **2004**, *84*, 4098.
[11] X. H. Kong, X. M. Sun, X. L. Li, Y. D. Li, *Mater. Chem. Phys.* **2003**, *82*, 997.
[12] J. Zhang, L. D. Sun, C. S. Liao, C. H. Yan, *Chem. Commun.* **2002**, 262.
[13] L. Vayssieres, K. Keis, A. Hagfeldt, S. E. Lindquist, *Chem. Mater.* **2001**, *13*, 4395.
[14] Z. Wang, H. L. Li, *Appl. Phys. A* **2002**, *74*, 201.
[15] H. D. Yu, Z. P. Zhang, M. Y. Han, X. T. Hao, F. Zhu, *J. Am. Chem. Soc.* **2005**, *127*, 2378.
[16] Q. C. Li, V. Kumar, Y. Li, H. T. Zhang, T. J. Marks, R. P. H. Chang, *Chem. Mater.* **2005**, *17*, 1001.
[17] S. J. Henley, M. N. R. Ashfold, D. P. Nicholls, P. Wheatley, D. Cherns, *Appl. Phys. A* **2004**, *79*, 1169.
[18] F. Claeyssens, C. L. Freeman, N. L. Allan, Y. Sun, M. N. R. Ashfold, J. H. Harding, *J. Mater. Chem.* **2005**, *15*, 139.
[19] D. M. Bagnall, Y. F. Chen, Z. Zhu, T. Yao, S. Koyama, M. Y. Shen, T. Goto, *Appl. Phys. Lett.* **1997**, *70*, 2230.
[20] E. C. Greyson, Y. Babayan, T. W. Odom, *Adv. Mater.* **2004**, *16*, 1348.
[21] X. Liu, X. Wu, H. Cao, R. P. H. Chang, *J. Appl. Phys.* **2004**, *95*, 3141.
[22] Y. Sun, G. M. Fuge, M. N. R. Ashfold, *Chem. Phys. Lett.* **2004**, *396*, 21.

Two-Polymer Microtransfer Molding for Highly Layered Microstructures**

By *Jae-Hwang Lee*,* *Chang-Hwan Kim*, *Kai-Ming Ho*, and *Kristen Constant**

Microfabrication techniques for highly layered microstructures have attracted much attention, since highly layered microstructures permit fabrication of three-dimensional (3D) devices with functionality not possible in planar devices. With the growing demands of highly layered microstructures for a number of applications, including artificial bones,[1,2] integrated microfluidic systems,[3–5] polymer-based integrated optical circuits,[6,7] photonic crystals,[8,9] and catalytic reactors,[10,11] reliable low-cost microfabrication methods are desirable. Traditional fabrication methods using photolithography are usually slow and costly. Over the last few years, a number of new approaches for fabricating 3D microstructures have been reported as alternatives to conventional photolithography such as microtransfer molding (μTM),[12] two-photon polymerization,[13,14] holographic lithography,[15,16] and nanoimprinting.[17] Among these techniques, μTM showed a number of advantages, including low cost, capability for non-periodic 3D structures, a wide range of materials compatibility, and flexibility in design. In conventional μTM, a liquid prepolymer fills microchannels formed on the surface of an elastomeric mold. The prepolymer is solidified after bringing the

[*] J.-H. Lee, Dr. C.-H. Kim, Prof. K.-M. Ho
Ames Laboratory–USDOE
and Department of Physics and Astronomy
Iowa State University, Ames, IA 50011 (USA)
E-mail: leejh@iastate.edu
Prof. K. Constant
Department of Materials Science and Engineering
Iowa State University, Ames, IA 50011 (USA)
E-mail: constant@iastate.edu

[**] This work is supported by the Director for Energy Research, Office of Basic Energy Sciences. The Ames Laboratory is operated for the U. S. Department of Energy by Iowa State University under contract No. W-7405-Eng-82.

 DOI: 10.1002/adma.200500721

ADVANCED MATERIALS

mold into contact with a substrate. Then, the structure is transferred to the substrate by removing the flexible mold. In spite of the many advantages of μTM, uncured filled prepolymer can smear out of the channels by capillary wicking when contacting a substrate. This wicking deteriorates structural fidelity and requires an additional processing step to remove the uncontrolled polymer, such as reactive-ion etching.[12] Partial curing of filled prepolymer is effective in avoiding capillary wicking since the partial curing increases the viscosity of the prepolymer;[12,18] however, uncured prepolymer is still favored to ensure sufficient bonding strength. Maximizing bonding strength, while minimizing the capillary wicking, is one of the most demanding technical challenges of this system.

We describe advanced μTM for highly layered microstructures, called two-polymer μTM (2P-μTM), with a residue-free filling method, sufficient bonding strength between layers for high yield, and extremely low capillary wicking for high structural fidelity. In 2P-μTM, we employ two different UV-curable prepolymers as a filler and an adhesive to avoid the difficulties of conventional μTM in which a single prepolymer performs both roles simultaneously. A schematic procedure of 2P-μTM is shown in Figure 1. We use PDMS molds cast from a master made out of a photoresist relief pattern on a silicon wafer.[19] A drop of the first prepolymer-A is placed just outside of a patterned area on a PDMS mold and dragged at a constant speed with a metal blade controlled by mechanical actuators. After dragging through the patterned area, the prepolymer-A only fills in the channels without any residue. We refer to this filling method as "wet-and-drag" (WAD). The filled prepolymer-A is partially cured so it solidifies, and the other prepolymer-B is subsequently coated only on the prepolymer-A by a second WAD. By placing a substrate on the mold and exposing to UV, the filled microstructure adheres to the substrate, and the structure remains on the substrate after peeling the PDMS mold away. By repeating the same sequential processes using a pre-stacked structure as a substrate, structures of any number of layers can be fabricated.

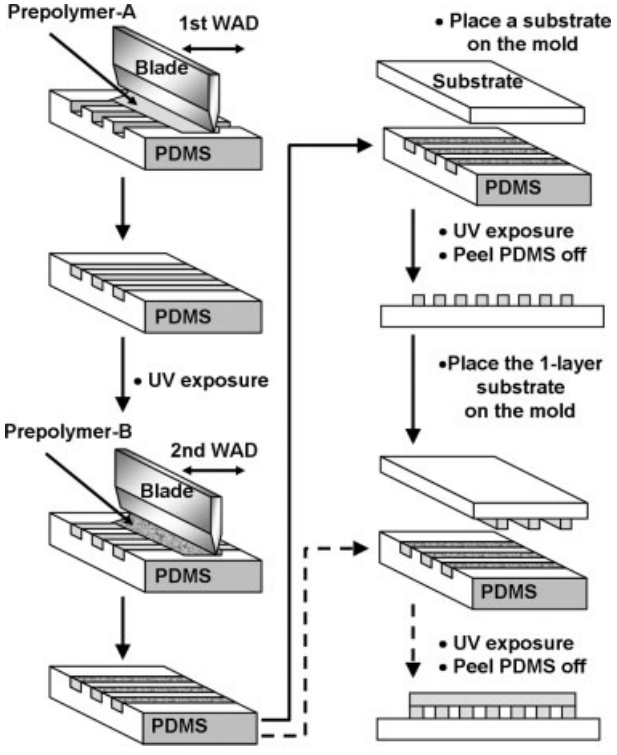

Figure 1. Schematic of two-polymer microtransfer molding procedure. PDMS: poly(dimethylsiloxane); WAD: wet-and-drag.

For the prepolymer-A, we tested a number of UV-curable prepolymers and found their viscosity affects the filling characteristics in WAD. For our patterned channels 1.4 μm wide and 1.1 μm deep, a polyurethane (PU) prepolymer, J-91 (Summers Optical), with a viscosity of around 300 cps, exhibits excellent filling characteristics. Lower- or higher-viscosity prepolymers caused uneven filling due to the rearrangement of the filled prepolymer within channels after WAD or formation of a thick layer over the channels, respectively. As a drop of PU is moved from a non-patterned area into a patterned area as shown in Figure 2a, empty channels (Fig. 2b) start to fill at a front boundary of the PU drop and all channels underneath of the drop of PU are completely filled. When the dragging of PU is continued, dewetting of PU on the top surface of the mold starts at the rear boundary of the PU drop. However, channels are left filled behind the dewetting line in Figure 2c because the adhesive energy of PU to the patterned PDMS surface exceeds the cohesive energy of PU. Figure 1d shows that PU completely fills the channels with a flat meniscus in Figure 1d.

Note that WAD is distinct from other coating methods using blades such as doctor blading in which the thickness of a film is related to the gap between a blade and a substrate. Because the role of the blade in WAD is only to control the macro movement of the prepolymer, filling properties are determined by the properties of the polymers and the shape of patterns formed on a mold, and not by the gap or the speed of the blade. The gap used was around 0.2 mm for better control of the movement of PU, and this value is about 200 times larger than the depth of channels being filled. This spontaneous dewetting characteristic allows WAD to produce residue-free filling and to avoid any physical damage or distortion of the PDMS mold by direct contact of the blade. When high-pressure nitrogen was used to remove excess prepolymers, we often observed tiny scattered droplets of prepolymers after blowing, which were very difficult to remove even using higher-velocity nitrogen. In contrast, residual prepolymer was not observed in the case of WAD. This may be because of the relatively low ability of PU to wet a non-patterned surface of PDMS (contact angle of around 72°). Although the range of applicable prepolymers is limited by the requirement of spontaneous filling, WAD can be complementary or alternative to other filling methods like scraping with a PDMS block, blowing off excess with inert gas, or conventional doctor blading. A dragging speed of around 30 $\mu m\,s^{-1}$ is selected because

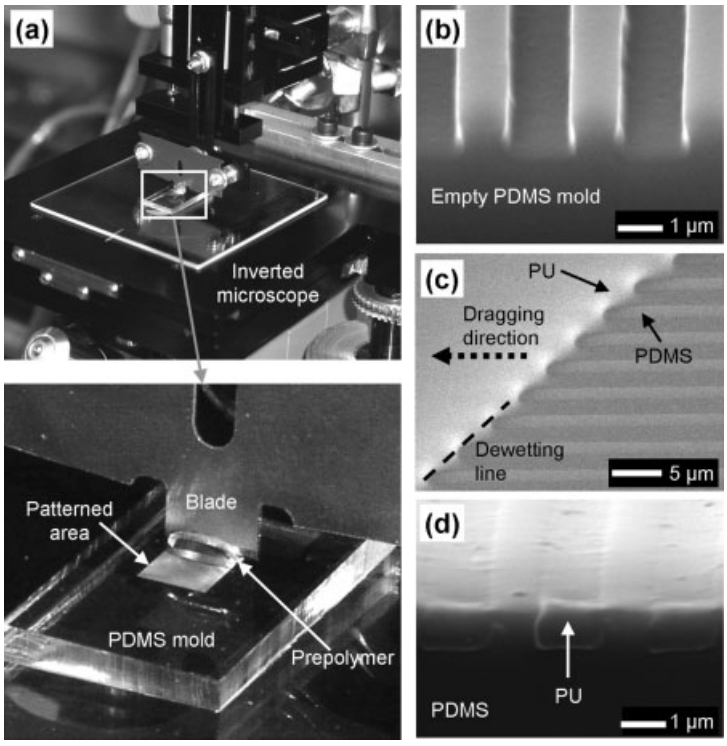

Figure 2. Photographs of the experimental setup and scanning electron microscopy (SEM) micrographs of WAD: a) Experimental apparatus for WAD; b) empty PDMS mold before WAD; c) boundary of a PU drop being dragged in WAD; d) filled PU in the channels after WAD. Note that PU in the images is fully cured for the SEM study.

faster or slower speeds cause a separation of prepolymer from the blade or more swelling of PDMS by PU, respectively. A single WAD of PU is sufficient to achieve residue-free, even filling through the entire 4 mm × 4 mm square area. This filling method is expected to be scalable to smaller dimensions.

For the polymer-B, a polymetacrylate prepolymer (PA), SK-9 (Summers Optical), is used, because PA satisfies several requirements as a bonding material: very low viscosity (80–100 cps) to form a thin layer; sufficient bonding strength to PU and glass; and a large surface-energy difference between PDMS and PU. The contact angles of PA on PU and PDMS are 8° and 54°, respectively. This difference provides the driving force for selective wetting. The second WAD with PA is performed on the PU-filled PDMS mold after solidifying PU by UV exposure. In WAD of PA, the gap of the blade is fixed at the same value, 0.2 mm, but the dragging speed is increased to 100 μm s^{-1} to minimize the swelling of PDMS by PA. The faster dragging speed is possible by virtue of the low viscosity of PA. Interestingly, a self-healing characteristic of WAD for PA was observed. The self-healing is achieved as more PA adheres around local defects on the PU surface. With the increased quantity of PA, the bonding strength around defects is significantly reinforced, preventing possible adhesion failure of the structures being transferred. The self-healing is indispensable to reduce failures because it confines defect sites locally. Otherwise, in some cases the detached structures generate global defects in the transferring of the next layer by hindering a contact.

Controlling the quantity of PA in the WAD process is critical for high yield. Insufficient or excess PA causes poor adhesion or an undesirable layer between the transferred structure and the substrate. Since each single layer in a fabricated multilayer structure consists of 1600 polymer rods, we simply define a transfer-error rate as dividing the number of transfer-failed rods by the total number of rods to be transferred. Here, we set the acceptable transfer-error rate as 10^{-4}. The transfer-error rate was much higher than the acceptable transfer-error rate when the PU filled in the PDMS mold was fully cured. We found that the transfer-error rate can meet the acceptable transfer-error rate by reducing the UV-exposure time of the PU. We theorize that dangling bonds in the polymer-network of the partially cured PU helps retain more PA. To determine the correlation between the UV dose for curing PU and the amount of coated PA, a red dye (LDS 698, Exciton) was added to PA. Here we assume that the intensity of photoluminescence from the doped dye is linearly proportional to the quantity of PA when the doping concentration of the dye is low (6×10^{-3} wt.-%). The dye doping does not appear to affect the functionality of the PA. After preparing PU-filled molds where the filled PU is exposed to different UV doses, WAD is performed with the dye-doped PA. Then, the photoluminescence intensities are measured, exciting the dye with an argon-ion laser ($\lambda = 514$ nm).

The correlation between the intensity of photoluminescence and the UV dosage is shown in Figure 3a. Here, we averaged all photoluminescence spectral values within 50 nm range around the photoluminescence peak as shown in Figure 3b. The relationship between the PA quantity and UV dosage to the PU is not monotonic; the intensity of photoluminescence shows a maximum at 0.9 J cm^{-2}. We do not consider dosages less than 0.2 J cm^{-2} because PU is apparently miscible with PA under an optical microscope when the dosage is less than 0.2 J cm^{-2}, showing PU still has much fluidity which would result in capillary wicking and structural deterioration at these lower dosages.

The transfer yield was sufficiently high to stack highly layered microstructures while satisfying the acceptable transfer-error rate for the dosage ranging from 0.45 to 2.7 J cm^{-2}. For doses outside this range, the transfer yield drops precipitously. In the acceptable range, the minimum dose, 0.45 J cm^{-2}, is considered the optimal UV dose for 2P-μTM because excess PA may result in an undesired thin film on a substrate, and a shorter curing time is better for reducing total process time. Note that the UV dose only represents the incoming dose from a UV source, not including the UV dose from reflected UV light by the interfaces of materials. The asymmetric photoluminescence spectrum in Figure 3b is mainly due to a low-pass filter, having a cut-off wavelength of 550 nm, used for blocking the excitation laser light.

ADVANCED MATERIALS

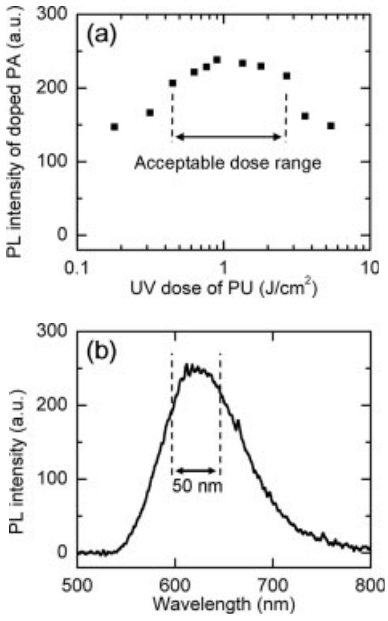

Figure 3. a) Photoluminescence intensity of dye-doped PA shows a correlation to the UV dose of PU. b) The photoluminescence spectrum, when the dose was 0.9 J cm^{-2}, with the range of averaging (50 nm). All other spectra showed a very similar spectral distribution.

If the area of PA application is wider than the area of transferred structures, it will hinder further processing. For instance, the excess film will hinder selective etching of substrates or electrodeposition using conducting substrates. To investigate the structure of the PA film and its bonding characteristics, we fabricated a two-layer structure on a glass substrate that was first coated with a water-soluble polymer. The dosage on PU was 0.45 J cm^{-2}. By dissolving the water-soluble polymer with distilled water, the two-layer structure was easily separated from its substrate, resulting in a free-standing form of the structure. The SEM images of the bottom surface of the separated structure are shown in Figure 4. In the micrographs, each bar shows quite clear edges without excess material. Interestingly, circular patterns, which were not observed before the WAD of PA in Figure 2d, were found at the bonding surface. Presumably, these patterns originated from air captured in making sudden contact with a substrate or the contraction of PA in curing. The flat disk-shaped remnants in Figure 4 confirm that the filled PU had lost its fluidity when placed on the substrate; otherwise hemispheric patterns would have been formed. From the patterns, we can infer that the PA coating is uniform and very thin as compared to the height of the PU bars.

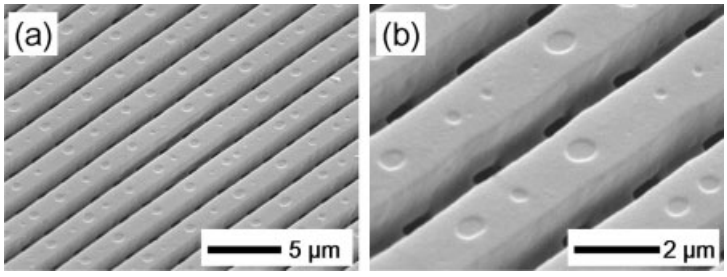

Figure 4. SEM images of bottom surface of transferred structure are shown with a) low and b) high magnification.

To demonstrate the feasibility of 2P-μTM for highly layered microstructures, we fabricated a 12-layer structure (Fig. 5) with the minimum acceptable dose, 0.45 J cm^{-2}. The area of the fabricated structure was 4 mm × 4 mm and the orientation of each layer was perpendicular to the one below. After fabrication, the 12-layer structure was cut along a 45° line to the orientation of each layer with a razor blade. The multilayer microstructure sustained this cutting with minimal damage, indicating a high bonding strength. Indeed, the high bonding strength is quite critical in the μTM technique because every bonding site of pre-stacked layers undergoes tensile stress whenever a PDMS mold is peeled away in transferring additional layers. Weakly bonded layers can debond at any stage in subsequent processing. The successfully fabricated 12-layer structure in Figure 5 indicates that each layer had sufficient bonding strength to withstand subsequent processing.

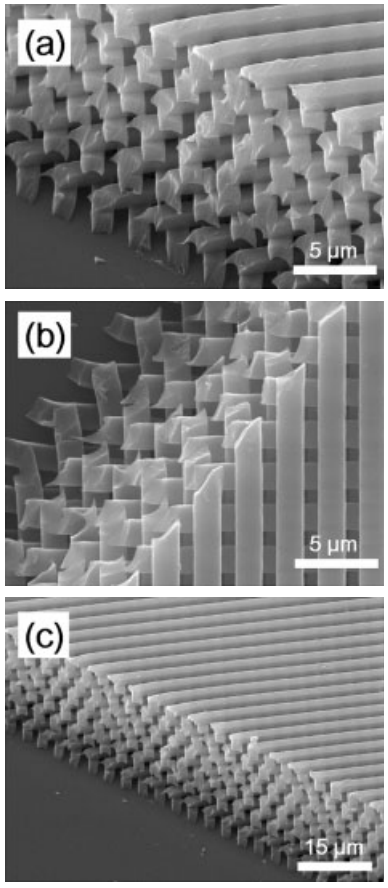

Figure 5. SEM images of the 12-layer microstructure: a) tilted view, b) top view, and c) lower magnification.

Note that the multilayer fabrication by using soft materials such as PDMS would have inherent limits in accuracy due to the irregular distortions of the soft materials used in processing. The distortion in 2P-μTM was investigated by using moiré-fringes metrology,[20] and the relative pattern mismatch was less than ±0.5 μm mm^{-1}. Although the inaccuracy from the distortions would limit the applications of 2P-μTM for large-area high-accuracy devices, it would still be tolerable for many other applications.

In conclusion, we developed 2P-μTM to provide a route for the fabrication of highly layered microstructures with high yield and high structural fidelity. We improved the consistency of the fabrication processes by controlling the UV dosage for the photocurable prepolymers. Applying two different prepolymers enable us to separate the bonding and the structural functions accomplished by a single prepolymer in conventional μTM. By separately controlling the chemistry and application of the prepolymers, we achieved both high bonding strength and extremely low capillary wicking. Moreover, exact filling without residues and selective coating of the prepolymer, relying on the differences in the surface energies, were efficiently achieved by WAD. We believe that the advantages of 2P-μTM will improve 3D microfabrication for a variety of applications while preserving the advantages of conventional μTM.

Experimental

PDMS Molding: We used a photoresist (AZ 5214, Clariant) relief pattern on a silicon wafer as a master pattern for PDMS molding. A two-component elastomeric kit, Sylgard 184 (Dow Corning), was used to make PDMS molds with the standard mixing ratio of base and hardener, 10:1 by weight. The mixture was poured on the master pattern and subsequently cured at 60 °C for 4 h. The thickness of the PDMS molds was about 2 mm in order to facilitate the peeling away of the PDMS molds.

UV Curing: In the experiment, a 100 W UV lamp was used with a high-pass filter and a beam homogenizer for 366 nm UV light. The UV-exposure system delivered a UV intensity of 1.5 mW cm^{-2} with a full width at half maximum of 4.8 nm. The ambient temperature of PDMS molds during the UV exposure was sustained at around 30 °C.

Photoluminescence Measurement: For the dye doping of PA, a red dye (LDS 698, Exciton) was dissolved in ethanol (4×10^{-3} mol-%). After mixing the ethanol solution of the dye with PA, the mixture was ultrasonically agitated for 5 h. The agitated mixture was purged with argon for 24 h at room temperature to remove ethanol. The doping ratio of the dye was 6×10^{-3} wt.-% after removal of ethanol. For consistent photoluminescence measurement, a hexagonally packed fiber bundle assembly, with the outer six fibers for excitation and the center fiber for detection, was used. To reduce the ependence of the detected photoluminescence intensity on the distance from a photoluminescence sample to the end tip of the fiber assembly, the distance was selected to be 20 times farther than the diameter of each fiber. Moreover, the distance was kept constant, within 0.2 % of the distance for each measurement, by optical means.

Received: April 8, 2005
Final version: May 23, 2005
Published online: September 1, 2005

[1] H. Kusakabe, T. Sakamaki, K. Nihei, Y. Oyama, S. Yanagimoto, M. Ichimiya, J. Kimura, Y. Toyama, *Biomaterials* **2004**, *25*, 2957.
[2] D. W. Hutmacher, *J. Biomater. Sci., Polym. Ed.* **2001**, *12*, 107.
[3] M. A. Burns, B. N. Johnson, S. N. Brahmasandra, K. Handique, J. R. Webster, M. Krishnan, T. S. Sammarco, P. M. Man, D. Jones, D. Heldsinger, C. H. Mastrangelo, D. T. Burke, *Science* **1998**, *282*, 484.
[4] P. F. Wagler, U. Tangen, T. Maeke, H. P. Mathis, J. S. McCaskill, *Smart Mater. Struct.* **2003**, *12*, 757.
[5] T. Thorsen, S. J. Maerkl, S. R. Quake, *Science* **2002**, *298*, 580.
[6] H. Ma, A. K.-Y. Jen, L. R. Dalton, *Adv. Mater.* **2002**, *14*, 1339.
[7] L. Eldada, L. W. Shacklette, *IEEE J. Sel. Top. Quantum Electron.* **2000**, *6*, 54.
[8] J. D. Joannopoulos, R. D. Meade, J. N. Winn, *Photonic Crystals: Molding the Flow of Light*, Princeton University Press, Princeton, NJ **1995**.
[9] S. Y. Lin, J. G. Fleming, D. L. Hetherington, B. K. Smith, R. Biswas, K. M. Ho, M. M. Sigalas, W. Zubrzycki, S. R. Kurtz, J. Bur, *Nature* **1998**, *394*, 251.
[10] I. Zuburtikudis, H. Saltsburg, *Science* **1992**, *258*, 1337.
[11] J. N. Stuecker, J. E. Miller, R. E. Ferrizz, J. E. Mudd, J. Cesarano, *Ind. Eng. Chem. Res.* **2004**, *43*, 51.
[12] X. M. Zhao, Y. Xia, G. M. Whitesides, *Adv. Mater.* **1996**, *8*, 837.
[13] H. B. Sun, S. Matsuo, H. Misawa, *Appl. Phys. Lett.* **1999**, *74*, 786.
[14] S. Kawata, H. B. Sun, T. Tanaka, K. Takada, *Nature* **2001**, *412*, 697.
[15] M. Campbell, D. N. Sharp, M. T. Harrison, R. G. Denning, A. J. Turberfield, *Nature* **2000**, *404*, 53.
[16] S. Shoji, S. Kawata, *Appl. Phys. Lett.* **2000**, *76*, 2668.
[17] L.-R. Bao, X. Cheng, X. D. Huang, L. J. Guo, S. W. Pang, A. F. Yee, *J. Vac. Sci. Technol., B: Microelectron. Nanometer Struct.—Process., Meas., Phenom.* **2002**, *20*, 2881.
[18] W. Y. Leung, H. Kang, K. Constant, D. Cann, C.-H. Kim, R. Biswas, M. M. Sigalas, K.-M. Ho, *J. Appl. Phys.* **2003**, *93*, 5866.
[19] A. Kumar, G. M. Whitesides, *Appl. Phys. Lett.* **1993**, *63*, 2002.
[20] J.-H. Lee, C.-H. Kim, Y.-S. Kim, K.-M. Ho, K. Constant, W. Leung, C. H. Oh, *Appl. Phys. Lett.* **2005**, *86*, 204 101.

Fabrication of PbS Nanoparticles in Polymer-Fiber Matrices by Electrospinning**

By *Xiaofeng Lu*, *Yiyang Zhao*, and *Ce Wang**

The synthesis of semiconductor nanoparticles, especially with diameters in the range 1–10 nm, is of considerable interest for potential exploitation of quantization effects for the preparation of optical signal processors and switches.[1–3] Size

[*] Prof. C. Wang, Dr. X. Lu, Dr. Y. Zhao
Alan G. MacDiarmid Institute, Jilin University
Changchun 130012 (P.R. China)
E-mail: cwang@jlu.edu.cn

[**] The financial support from the Major International Collaborative Project of National Natural Science Foundation of China (Grant 20320120169), the National Major Project for Fundamental Research of China (National 973 Program No. 001CB610505), and the National Nature Science Foundation (50473007 and 50473008) is greatly appreciated.

 DOI: 10.1002/adma.200500196